Theor. Appl. Climatol. 78, 123–135 (2004)
DOI 10.1007/s00704-004-0048-5

Theoretical and Applied Climatology
Printed in Austria

[1] Department of Atmospheric Sciences, Institute of Astronomy, Geophysics and Atmospheric Sciences, University of São Paulo, São Paulo, Brazil
[2] Department of Meteorology, Federal University of Pará, Belém, Brazil

Simulation of deforestation in eastern Amazonia using a high-resolution model

A. W. Gandu[1], **J. C. P. Cohen**[2], and **J. R. S. de Souza**[2]

With 11 Figures

Received December 10, 2002; revised July 8, 2003; accepted October 24, 2003
Published online April 20, 2004

Summary

This work evaluates the impact of deforestation on the climate of the eastern portion of the Amazon basin. This region is primarily an area of native tropical rainforest, but also contains several other natural ecosystems such as mangroves and savanna. It is the most densely populated area in Amazonia, and has been significantly affected by deforestation. In this study, numerical simulations were performed with a high spatial resolution, regional model that allows for consideration of mesoscale aspects such as topography, coastlines and large rivers.

To evaluate the present situation and to predict potential future effects of deforestation on the climatic conditions of this region, two, one-year model simulations were made. In the first, ''control simulation'', an attempt was made to match the existing surface vegetation. The biophysical parameters used were derived from recent studies of similar Amazon-region ecosystems. In the second run, ''deforested simulation'', the forested-area biophysical parameters were replaced by those corresponding to the pasture areas of the region.

The higher-resolution regional modelling revealed important climatic features of the deforestation process, displaying some associated mesoscale effects that are not typically represented in similar Global Circulation Model simulations. Near coastal zones and along large rivers, deforestation resulted in reduced cloud cover and precipitation. However, increased cloud cover and precipitation was predicted over upland areas, especially on slopes facing river valleys. The modelled surface sensible and latent heat fluxes also presented both positive and negative anomalies. The magnitudes of these anomalies were greater during the dry season. Windspeed near the surface was the meteorological variable that presented the most significant change due to deforestation. The reduction in roughness coefficient resulting from the shift from forest to pasture produced increased windspeeds near the Atlantic coast. The greater windspeeds diminished local humidity convergence and consequently reduced rainfall totals in nearby regions.

The results obtained from these higher-resolution simulations show that, in general, orography, coastline profile and the distribution of large rivers play important roles in determining anomaly patterns of precipitation, wind, and energy exchange associated with deforestation in eastern Amazonia.

1. Introduction

Evaluating the potential impact of Amazonian deforestation on precipitation is critical to understanding how the local hydrological cycle may change in the future. This type of study can also improve understanding of the remote effects of Amazonian deforestation and precipitation on weather and climate in other regions of the world (Eltahir, 1996; Werth and Avissar, 2002). One of the most active areas of deforestation is eastern Amazonia. This region is complex and comprises various ecosystem types, such as native and regrowth forests, mangroves, savannas, natural fields, pasture fields and agricultural areas. The region is characterised by proximity to the

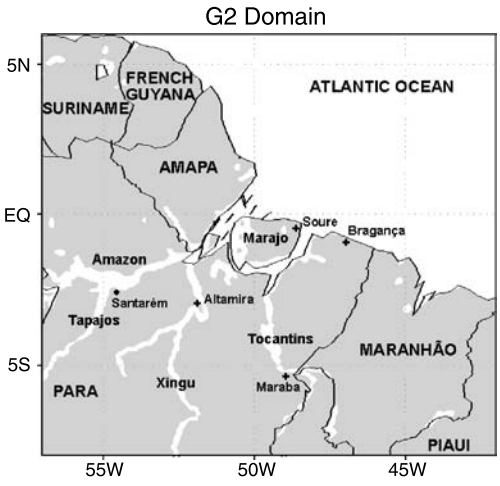

Fig. 1. Fine-grid map of the modelled region showing principal rivers, state boundaries and major cities. Cities indicated with a cross are those with ground level automatic stations that recorded the precipitation data used in comparisons between actual precipitation levels and those simulated in the control run

Atlantic Ocean and by the presence of large rivers: the Tapajós, the Xingú, the Tocantins and the Amazon which merge in an area of major confluence around Marajó Island (Fig. 1). Moving westward along the River Amazon, several other great rivers and flood plains are found in the western portion of the State of Pará, beyond the River Tapajós, in the areas surrounding the city of Santarém. This unique physiography, characteristic of the region, combined with large-scale atmospheric circulation and intense water vapour flux from the Atlantic, makes eastern Amazonia one of the rainiest regions on Earth. This has a definite effect on biodiversity and commercial land use in the area.

The seasonal climatic cycle in eastern Amazonia is heavily influenced by the north–south migration of the Intertropical Convergence Zone (ITCZ) (Horel et al., 1989). The timing of this migration determines the arrival of the period of heaviest rainfall, sometime between January and April, as well as that of the dry season, occurring between September and November (Rao and Hada, 1990; Figueroa and Nobre, 1990). The onset of the rainy season in this region is associated with enhancement of the northern component of the meridional wind (Wang and Fu, 2002) and attenuation of the easterly-wind zonal component (Marengo et al., 2001).

Although the characteristics of the atmosphere over eastern Amazonia are determined by the large-scale circulation, the proximity of the ocean and the large rivers creates area-specific spatial and temporal precipitation variabilities. These values are clearly modulated by maritime-breeze circulations (Kousky, 1980) and by river breezes (Silva Dias et al., 2004). For example, the mesoscale circulation associated with the maritime breeze may organise the convection into coastal squall lines, which are responsible for a significant portion of the precipitation in this region (Garstang et al., 1994; Cohen et al., 1995). The interaction between the large-scale circulation and the maritime-breeze circulation also determines the time of day for the precipitation events on the north-eastern coast of South America (Kousky, 1980; Negri et al., 2000).

Several Global Circulation Model (GCM) studies have evaluated the local and regional climatic impact of the complete substitution of Amazonian forest by pasture (Nobre et al., 1991; Polcher and Laval, 1994; Lean et al., 1996; Manzi and Planton, 1996; Hahmann and Dickinson, 1997; Costa and Foley, 2000). In general, these studies indicate that total replacement of forest by pasture will result in a hotter, drier climate in the region (see, for example, Table 1 in Hahmann and Dickinson, 1997). On the other hand, some results from GCM simulations show contradictory effects, suggesting that these models are highly sensitive to the physical processes they represent. Sensitivity of large-scale tropical convection to alterations in landscape has been investigated by Polcher (1995). Employing a conceptual model of convection dynamics, Polcher suggested that the variations found in his studies of tropical deforestation could be explained by changes in the frequency of intense convective events. He concluded that this phenomenon occurs primarily because these events are highly sensitive to sensible heat fluxes at the surface.

A regional numerical study of the climatic effects of deforestation in Amazonia has been performed by Silva Dias and Regnier (1996). However, their focus was on the state of Rondônia, in the western region of Brazil. No detailed numerical studies have yet been performed for eastern Amazonia, for which, the simulations are likely to be quite different than those presented for western Amazonia.

The climatic effects of large-scale deforestation are attributable to the complex interactions

Table 1. Biophysical parameters for each category of vegetation used

Parameter	Forest	Pasture	*Cerrado**
Albedo	0.13(1)	0.18(1)	0.18(2)
Emissivity	0.95	0.96	0.97
Leaf area index (LAI)	5.2(1)	2.7(1)	1.0(2)
LAI seasonal variation	1.0	2.0	0.8
Vegetation fraction coverage (Vfrac)	0.98(3)	0.85(3)	0.50
Vfrac seasonal variation	0.05	0.10	0.30
Roughness length, z_o (m)	2.35(1)	0.05(1)	1.20(2)
Zero plane displacement (m)	28.4(1)	0.3(1)	10.0(2)
Root depth (m)	4.0(1)	1.0	2.0
Stomatal conductance ($mm\,s^{-1}$)	0.0035(4)	0.0010(4)	0.0020(4)

* Savanna-like vegetation

Superscripts refer to the source references as follows: (1) Wright et al., 1996; (2) Miranda et al., 1996; (3) Silva Dias and Regnier, 1996; and (4) Freitas, 1999

of soil and vegetation, energy and water exchanges, cloud formation and general atmospheric circulation. On a smaller scale, significant orography and local circulation caused by the proximity of the ocean and of large rivers may also contribute to the local characteristics of temperature, energy fluxes and surface distribution of precipitation. Predictions of the potential effects of further deforestation, derived from numerical simulations, are highly dependent upon the model used, as well as upon the radiation balance, precipitation, air temperature, diffusivity and other physical parameters adopted (Manzi and Planton, 1996).

The objective of this study was to simulate the atmospheric effects of total substitution of forest by pastureland in the eastern region of Amazonia. In order to achieve higher spatial resolution, the Regional Atmospheric Modelling System (RAMS) model was used. The general characteristics and configurations of the version of the RAMS model chosen are presented in Section 2 of this paper. In addition, the initial conditions, lateral conditions and surface boundary conditions selected for ''control'' and ''deforested'' simulations are specified. The simulated results, in which surface variables are analysed in terms of annual averages and seasonal-scale, specified-period averages, are presented in Section 3. The final summary and the conclusions are found in Section 4.

2. Experimental design

The RAMS model employed is a comprehensive numerical model of the atmosphere and includes prognostic equations for temperature, water vapour, liquid water (cloud and rain), three wind components and five species of ice forms (Tripoli and Cotton, 1982; Tremback, 1990; Walko et al., 1995). The RAMS model has been widely used to simulate relatively short-term (hours to several days) atmospheric and land-surface processes (Pielke et al., 1992), and, more recently, to simulate climate (Liston and Pielke, 2001; Lu et al., 2001). The model version used in this work was Version 4.4. An overview of the model characteristics is given by Cotton et al. (2003).

In this study, the model was configured with two grids. The first had 22 east–west points and 17 north–south points (horizontal interval between points: 200 km) and encompassed an area from latitude 14° S to 14° N and from longitude 26° W to 64° W. The second grid, nested within the first, had 38 east–west points and 34 north–south points (horizontal interval between points: 50 km). This second grid covered the region which includes the countries of Suriname and French Guyana and the Brazilian states of Amapá and Pará, Maranhão (in large part), Tocantins (northern portion) and Piauí (western portion) (Fig. 1). Both grids had 25 vertical layers, the first of which encompassed the initial 100 m of atmosphere. Each successive layer increased by a factor of 1.2 until attaining a dimension of 1000 m. Continuing up to the model top (22.6 km), all subsequent layers were 1000 m thick. The model uses physical variables of 12 soil layers, with the bottom of each layer at the following levels (in metres): 0.01, 0.03, 0.05, 0.10, 0.15, 0.20, 0.30, 0.50, 1.0, 2.0, 3.0, and 4.0.

The model topography was defined using the global, 30 arc-second, latitude–longitude dataset

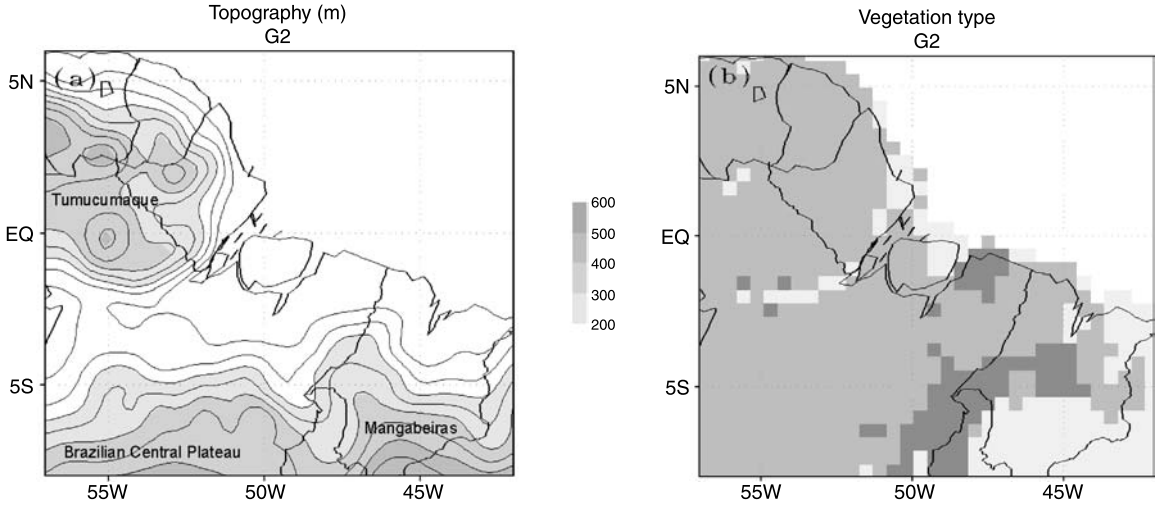

Fig. 2. (**a**) Fine-grid topographical map of the modelled area, showing the principal upland regions. Contour intervals are 50 m, with a minimum altitude of 100 m and shaded after 200 m. (**b**) Fine-grid map of vegetation distribution. Dark, medium and light shading correspond to ''pasture'', ''forest'' and ''cerrado'' areas, respectively

available through the United States Geological Survey's (USGS) Earth Resources Observation System (EROS). The topographic distribution for the fine grid is shown in Fig. 2a. Within the grid, there were some important areas of higher elevation such as the Tumucumaque mountain chain (in north-western Pará, west of Amapá and south of French Guyana and Suriname), the Brazilian central plateau (in southern Pará) and the Mangabeiras high flats (in southern Maranhão). The topography in the central portion of the fine grid is dominated by lowlands that begin on Marajó Island on the Atlantic coast and follow the Amazon valley to the western and south-western sectors.

The RAMS sub-model that simulates interactions between soil, vegetation and atmosphere uses the land-to-water area ratio in each grid cell of the model to compute the sensible and latent heat fluxes (Walko et al., 2000). In this study, the land-water fraction used was derived from the ''vegetation types'' data files produced by the Centro de Previsão de Tempo e Estudos Climáticos (CPTEC) of the Instituto Nacional de Pesquisas Espaciais (INPE) (Sestini et al., 2002).

The vegetation-cover distribution data used for the fine grid were also taken from the CPTEC/INPE data files and are shown in Fig. 2b. The region presents a great variety of vegetation types and, in order to simplify this study, the different types of vegetation in this domain were classified as either ''forest'', ''pasture'' or ''cerrado'' (a type of savanna). According to this classification, the major portion of the continental region within the modelled domain is covered by forest. The cerrado types of vegetation are found mainly in the southern areas of Maranhão and Piauí, on the eastern side of Marajó Island, along the eastern coast of Amapá and in some spots along the Amazon. The areas already deforested are more significant in south-eastern Pará and in the central region of Maranhão. A smaller area representative of this type of vegetation is also found on the north-eastern coast of Pará, on the eastern side of Marajó Island.

The original RAMS biophysical parameters for each type of vegetation were replaced (Table 1) by either locally observed values (Wright et al., 1996; Miranda et al., 1996) or by those adopted in previous studies of Amazonia (Silva Dias and Regnier, 1996; Freitas, 1999). Values not indicated by the index in Table 1 were assumed in accordance with a personal communication from Humberto da Rocha.

Two simulation runs were performed. In the first (CONTROL), each vegetation class within the modelled domain was given its proper biophysical parameters, according to Table 1. In the second simulation (DEFORESTED or NOFOR), the vegetation biophysical parameters of the ''forest'' classification were replaced by the

respective biophysical parameters of the ''pasture'' classification.

Both simulations were initialised with geopotential, temperature, relative humidity and horizontal wind components obtained from the National Centers for Environmental Prediction (NCEP) global model analysis. Analysis was at standard pressure levels, using a grid of 2.5° latitude by 2.5° longitude. The lateral boundary conditions for the coarse grid were also provided by the NCEP model analysis and were assimilated at each grid limit point, with a nudging time of 900 seconds. Sea surface temperature (SST) was defined on a 1° global grid according to the National Oceanic and Atmospheric Administration (NOAA) weekly analysis and was interpolated to find the SST values for this RAMS model simulation.

In setting initial conditions for temperature in all soil layers, it was assumed that values were 6 °C higher than those established at the first level of the atmospheric model. This soil temperature/air temperature differential is the median for the month of August in this region (Souza et al., 2002). The initial conditions for the horizontally non-homogeneous soil moisture contents were derived from climatology data for the month of August (Rossato et al., 2002).

The model runs spanned a 13-month period, starting at 00 h UTC on 1 August 2000 and ending at 00 h UTC on 1 September 2001. The results shown and discussed relate to regional averages of one-year periods and three-month periods. The three-month averages correspond to the periods of heaviest rainfall (February to April) and least rainfall (June to August) observed over the course of this study.

3. Results

Several previous studies have documented the annual variation and spatial distribution of rainfall in the Amazon basin (Figueroa and Nobre, 1990; Marengo, 1992; Rao et al., 1996). The relationship between precipitation and large-scale circulation has also been investigated (Horel et al., 1989; Hastenrath, 1997). Eastern Amazonia has one of the highest annual rainfall rates in the world. The Amapá coast and Amazon delta receive more than 3000 mm of precipitation per year. Interior regions, such as the central and western portions of the state of Pará, receive approximately 2000 mm annually. The greater part of this precipitation falls during the period between January and April, due to the southward movement of the ITCZ.

In Fig. 3, both actual and simulated monthly precipitation averages are shown for the period of September 2000 to August 2001. Measurements of actual precipitation were taken at automatic meteorological stations, two on the coast (at Soure and Bragança) and two in the interior

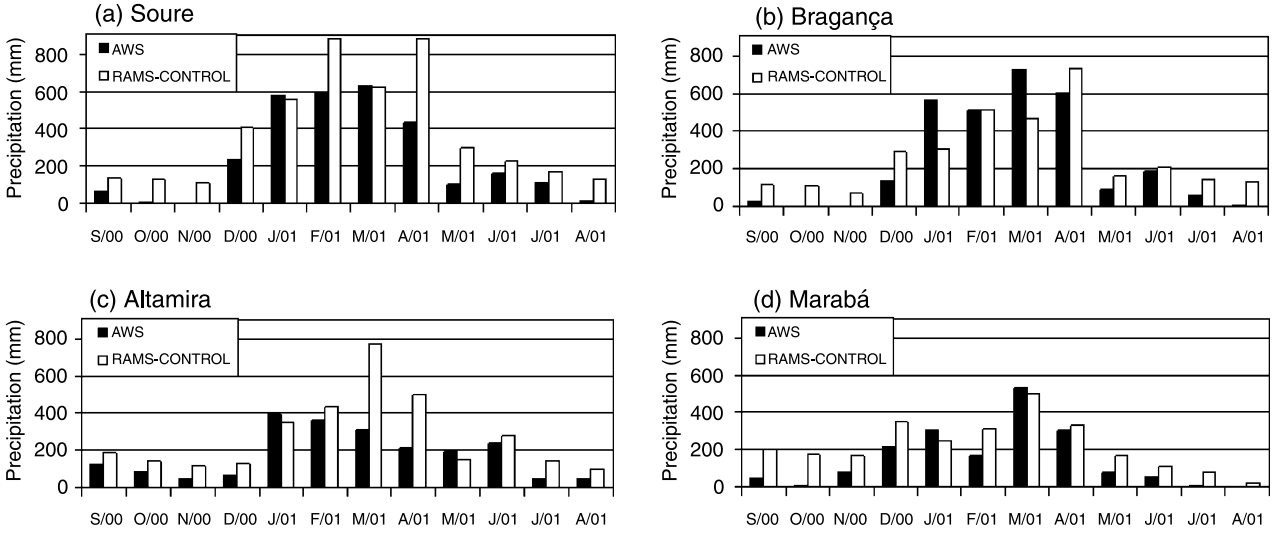

Fig. 3. Comparison of monthly precipitation (mm) collected between September 2000 and August 2001 at the ground level automatic stations (indicated in Fig. 1) with that simulated in the control run for the same period

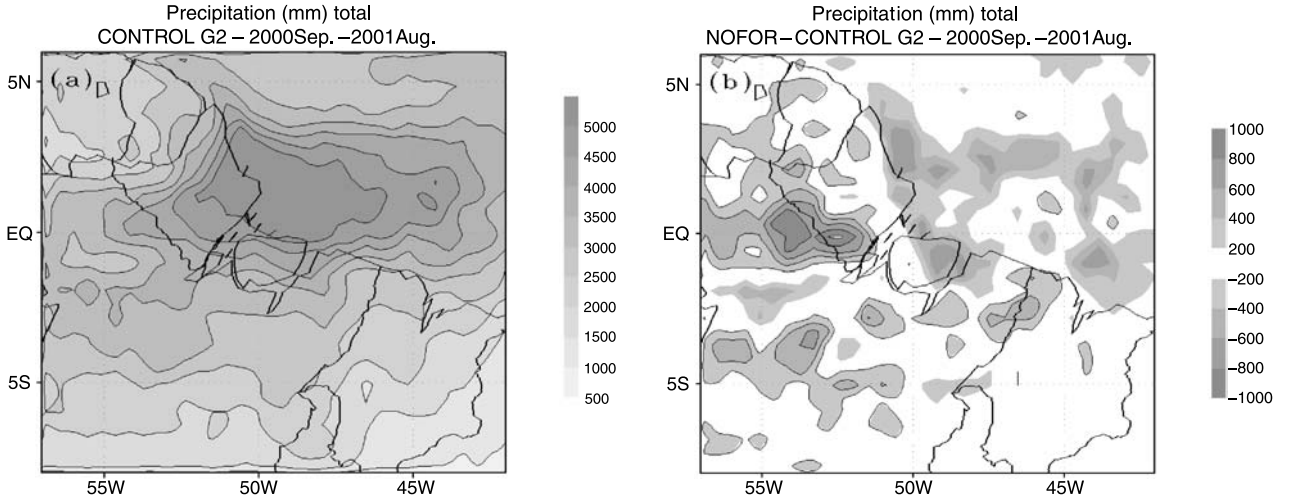

Fig. 4. Total (convective plus microphysics) accumulated precipitation fields (mm) for: **a**) 12-month control run and **b**) anomaly (deforested minus control). Contour intervals are 500 mm (**a**), and 200 mm (**b**). Solid contours for positive values (**b**)

(at Altamira and Marabá). The simulated monthly averages shown are those from control runs for the same stations. Disregarding a few anomalous months, comparison of observed precipitation and simulated precipitation shows that the control run simulation was able to capture the annual precipitation cycles in the region relatively well. Taking eastern Amazonia and the adjacent Atlantic coastal waters as a whole, the control run also succeeded in simulating the annual north–south movement of the ITCZ (Fig. not shown.).

Control-run precipitation totals accumulated during the 12 months, September 2000 to August 2001, are shown in Fig. 4a. Despite the apparent agreement between the observed and simulated distribution patterns, it is important to note that simulated precipitation values were overestimated. There is a large area of maximum precipitation encompassing the coastal area of Amapá, the Amazon delta, the northern part of Marajó Island and a portion of the adjoining coastal waters. Precipitation values in RAMS simulations were arrived at by summing precipitation values generated by the microphysics RAMS module (commonly known as ''explicit microphysics precipitation'' or ''totpcp'') and those generated by Kuo cumulus parameterisations (known as ''convective precipitation'' or ''acccon''). Precipitation distribution patterns simulated by the control run were primarily determined by the microphysics module, accounting for 85% of all simulated precipitation.

The total precipitation field shown in Fig. 4a displays a smaller but significant area of maximum precipitation along the Amazon valley. The higher precipitation values for this area, especially the rainy-season values, can also be attributed to the microphysics module.

The anomalies in annual accumulated precipitation totals resulting from the NOFOR simulation minus the CONTROL values are shown in Fig. 4b. The data shown indicate that, if the forest were replaced by pasture, there would be a definite precipitation reduction in certain areas. A coastal area stretching from Amapá to the eastern portion of Marajó Island, as well as an east–west strip of the Atlantic, would suffer an approximate 16% reduction in precipitation. The coastal area of negative precipitation anomaly may be attributed to a reduction in water vapour convergence near the ocean, owing to the changes in vegetation. As the surface roughness coefficient decreased, there would be an increase in windspeed over those areas, with the attendant reduction in humidity convergence.

Another area, in and around the River Amazon city of Santarém, would see precipitation totals decrease by approximately 10% after the substitution of forest by pasture. This reduction was almost entirely generated by the microphysics module (Fig. 5a) and would be observed in both dry and rainy seasons.

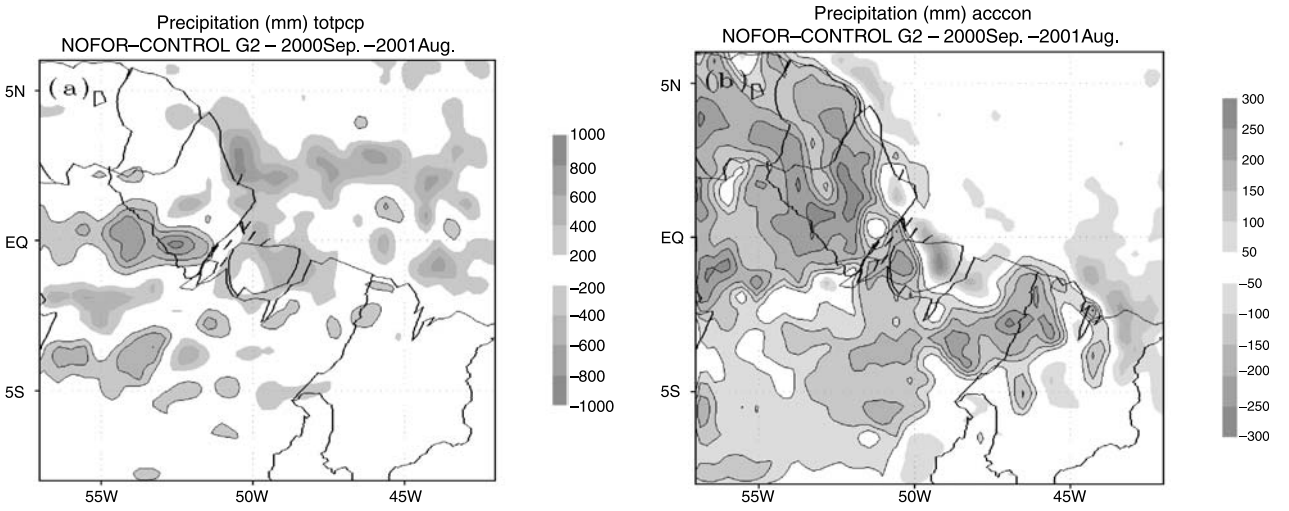

Fig. 5. Annual precipitation anomaly (deforested minus control), in mm, for: **a**) explicit microphysics precipitation and; **b**) parameterised convective precipitation. Shading intervals are 200 mm (**a**), and 50 mm (**b**). Solid contours for positive values

Contrary to most previous studies, which used GCM atmospheric simulations, the precipitation field anomalies in the present simulations also showed areas of enhanced precipitation, constituting positive anomalies of some 10 to 16% (Fig. 4b). As can be seen, these anomalies were primarily on the slopes of the uplands to the north and south of the River Amazon. Both microphysics (Fig. 5a) and parameterised convective rainfall (Fig. 5b) contributed to the calculation of these precipitation increases. At higher altitudes, the latter predominated.

Consistent with the precipitation behaviour, cloud cover over the coastal areas of Amapá and along the River Amazon reduces by approximately 5% after deforestation (Fig. 6). In this region, the reduction in cloud cover is more evident during the dry season (Fig. 6b). Conversely, an increase in cloud cover was observed over the upland slopes of the region, both during the rainy period (Fig. 6a) and during the dry period (Fig. 6b).

The annual anomalies in sensible heat flux distribution (Fig. 7a) present only a few differences between the CONTROL and NOFOR runs for

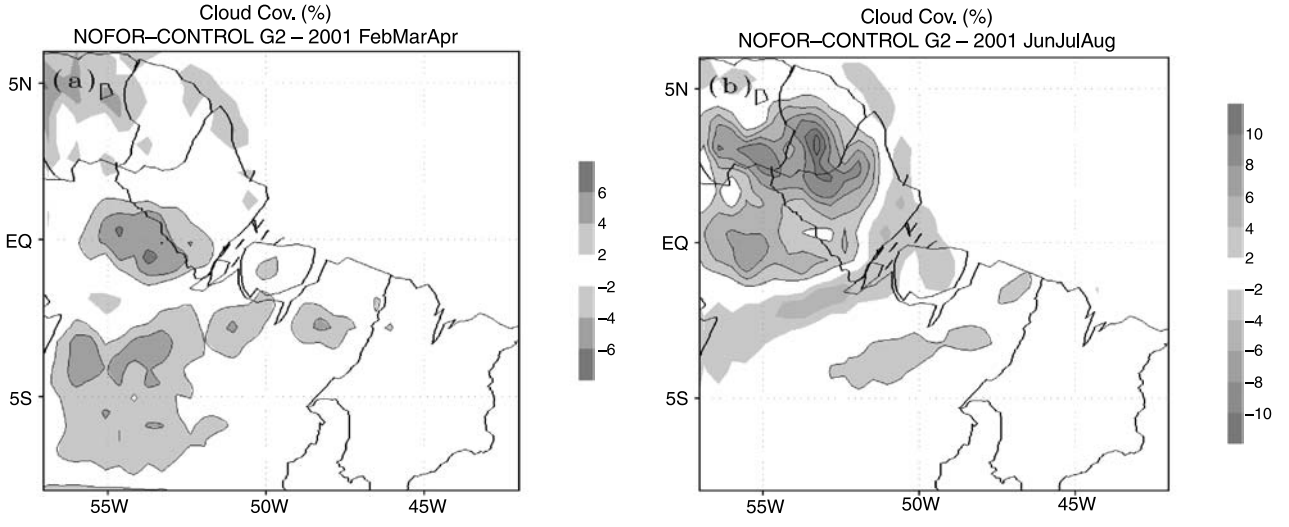

Fig. 6. The cloud-cover anomaly (deforested minus control), in %, for: **a**) February to April 2001 and; **b**) June to August 2001. Shading intervals of 2%. Solid contours for positive values

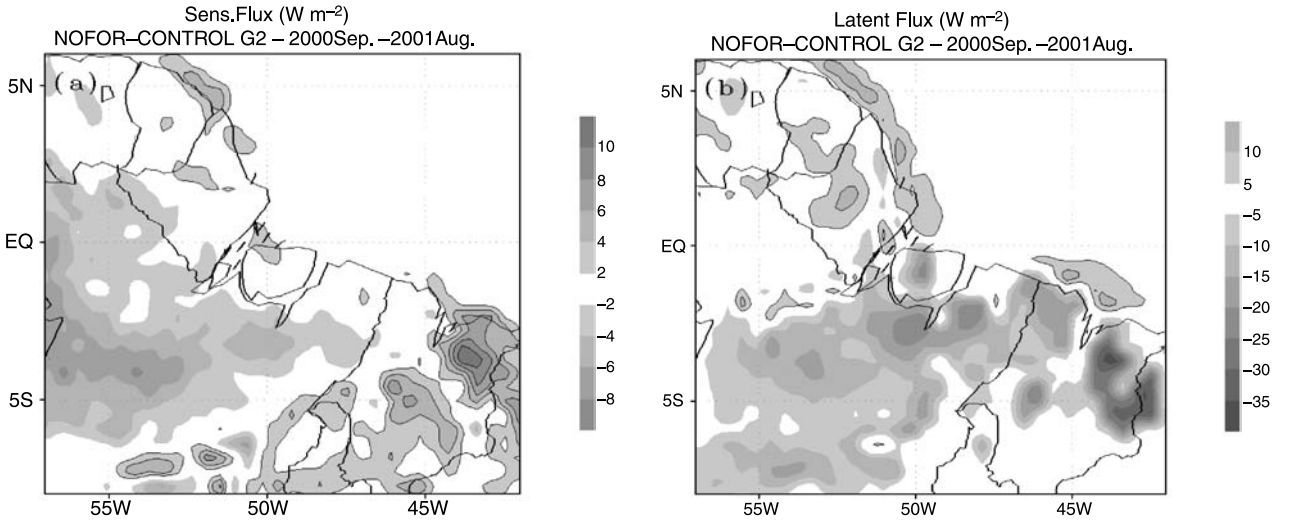

Fig. 7. Annual anomaly (deforested minus control) of: **a**) surface sensible heat flux ($W\,m^{-2}$); and **b**) surface latent heat ($W\,m^{-2}$). Shading intervals are $2\,W\,m^{-2}$ (**a**), and $5\,W\,m^{-2}$ (**b**). Solid contours for positive values

the coastal area extending from Amapá and Marajó Island to north-eastern Pará and north-western Maranhão. Nevertheless, over more continental areas, the substitution of forest by pasture produced an attenuation of approximately 10% in sensible heat flux values, consistent with findings from previous studies (Manzi and Planton, 1996). In the simulated dry months, this attenuation was more pronounced (Fig. 8a). In the southern and south-eastern sections of the modelled domain, an increase in sensible heat flux can be seen within an area dominated by cerrado-type vegetation.

The latent heat flux anomaly distribution (Fig. 7b) indicates an attenuation of nearly 6% in the central, southern and north-eastern regions of Pará. There is a more intense negative anomaly nucleus in north-eastern Maranhão, extending into the state of Piaui. In contrast, the same substitution of forest by pasture resulted in an enhancement of latent heat fluxes over the upland region north of the equator (Fig. 8b). During the dry period in the modelled domain, both positive and negative latent heat flux anomalies occur. The absolute values of these anomalies are comparable to those estimated by previous studies

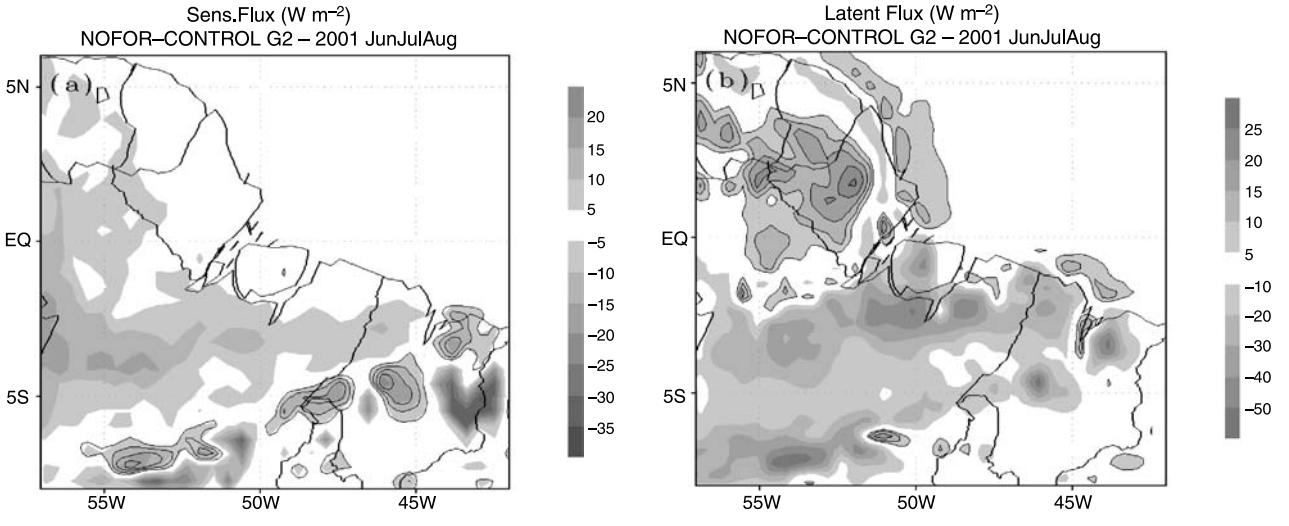

Fig. 8. The dry quarter (June to August 2001) average anomaly (deforested minus control) of: **a**) surface sensible heat flux ($W\,m^{-2}$) and; **b**) surface latent heat flux ($W\,m^{-2}$). Shading intervals are $5\,W\,m^{-2}$. Solid contours for positive values

(Manzi and Planton, 1996; Hahmann and Dickinson, 1997).

It is of note that replacement of forest by pasture over the continent leads to an approximate 6% increase in latent heat fluxes over the ocean, near the Amapá and Maranhão coasts (Figs. 7b and 8b). This increase occurs as a result of increased windspeed at the ocean-continent interface, due to the difference in roughness coefficient between forest and pasture values. In this model, evaporation over the ocean depends on SST and windspeed. The same SST was adopted in the two model runs and the model had no coupled ocean module capable of changing the SST according to vertical mixing. Therefore, the increase in windspeed inevitably led to higher local latent heat fluxes.

Over the modelled domain, the effects of deforestation on temperature and water vapour field distributions were more pronounced during the dry season. Therefore, only the results corresponding to the period from June to August are presented (Fig. 9). For the first simulated atmospheric level (altitude, 47 m), the average temperature anomaly during this quarter (Fig. 9a) showed an increase of about 1 °C over most of the land surfaces within the domain. The nucleus of a higher temperature anomaly was identified over the upland areas of Amapá. Along the Amazon and in the flood plains around Santarém, temperatures showed little variation due to deforestation. Over regions that presented positive temperature anomalies, a decrease of approximately $0.5\,g\,kg^{-1}$ in the water vapour mixing ratio was observed (Fig. 9b). Lesser variations in this ratio were found along the Amazon and in the coastal areas of Amapá and Pará.

Among all meteorological variables considered, the greatest variation was seen in windspeed at the first level of the model (Fig. 10). Inland, near the coast, windspeed was predicted to increase by approximately 80% after deforestation. The windspeed would rise from 3.0 to $5.5\,m\,s^{-1}$, mainly over upland slopes in Amapá and near the border between Pará and Maranhão. The nuclei of maximum windspeed variations were positioned mainly over the up-wind sides of the ranges of hills nearer to the Atlantic coast. Such is the case over the State of Amapá, especially during the rainiest months (Fig. 10a), when the prevailing winds are from the north–east. It is also the case around the border between Pará and Maranhão during the drier months (Fig. 10b), when the prevailing winds are from the east.

It should be noted that the smallest post-deforestation variations in windspeed were predicted along the Amazon, a river which, coincidentally, flows in the same direction as the prevailing winds. The contrast between the minimal variations in windspeed along the Amazon and the more pronounced variations in other regions was more evident during the local dry season

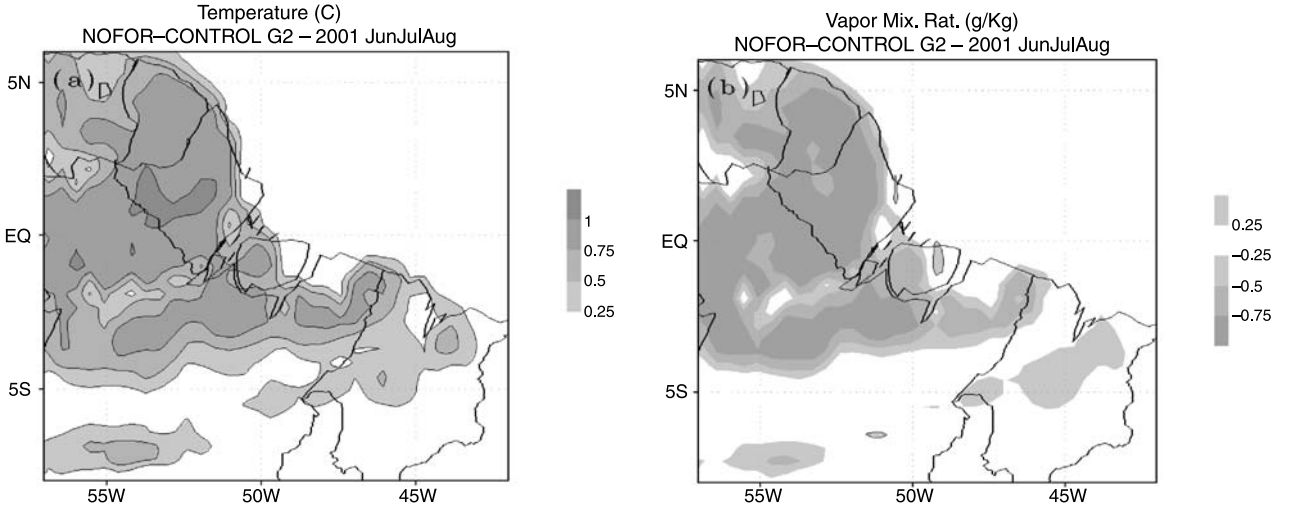

Fig. 9. The dry quarter (June to August, 2001) averages for: **a**) temperature anomaly (deforested minus control) in °C and; **b**) water vapour mixing ratio anomaly (deforested minus control) in $g\,kg^{-1}$. Shading intervals are 0.25 °C (**a**), and $0.25\,g\,kg^{-1}$ (**b**). Solid contours for positive values

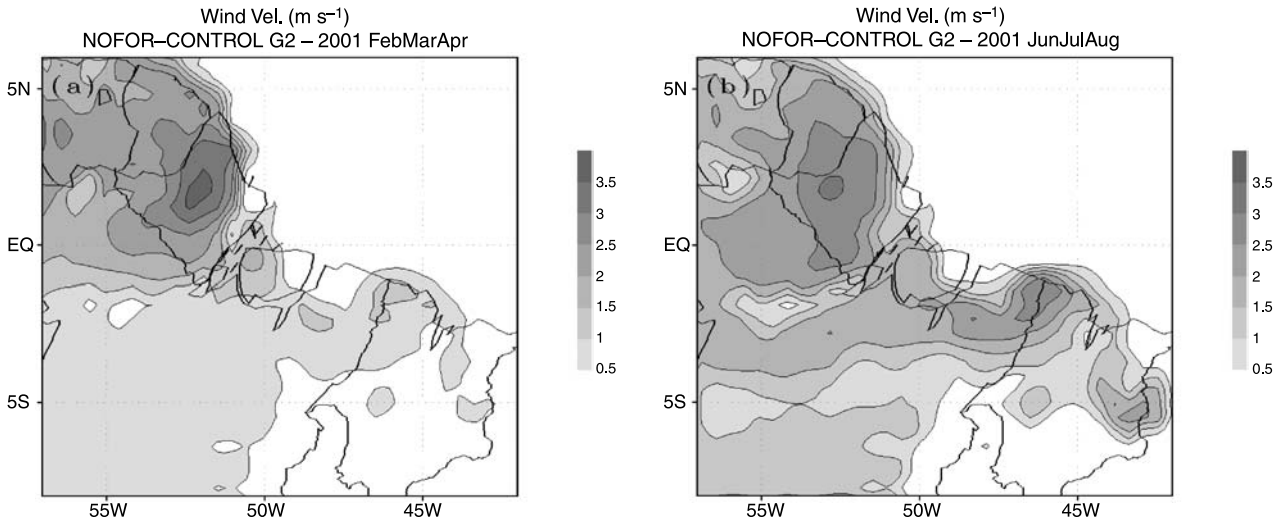

Fig. 10. The average windspeed anomaly (deforested minus control), in $m\,s^{-1}$, for: **a**) rainy months (February to April 2001) and; **b**) dry months (June to August 2001). Shading intervals are $0.5\,m\,s^{-1}$. Solid contours for positive values

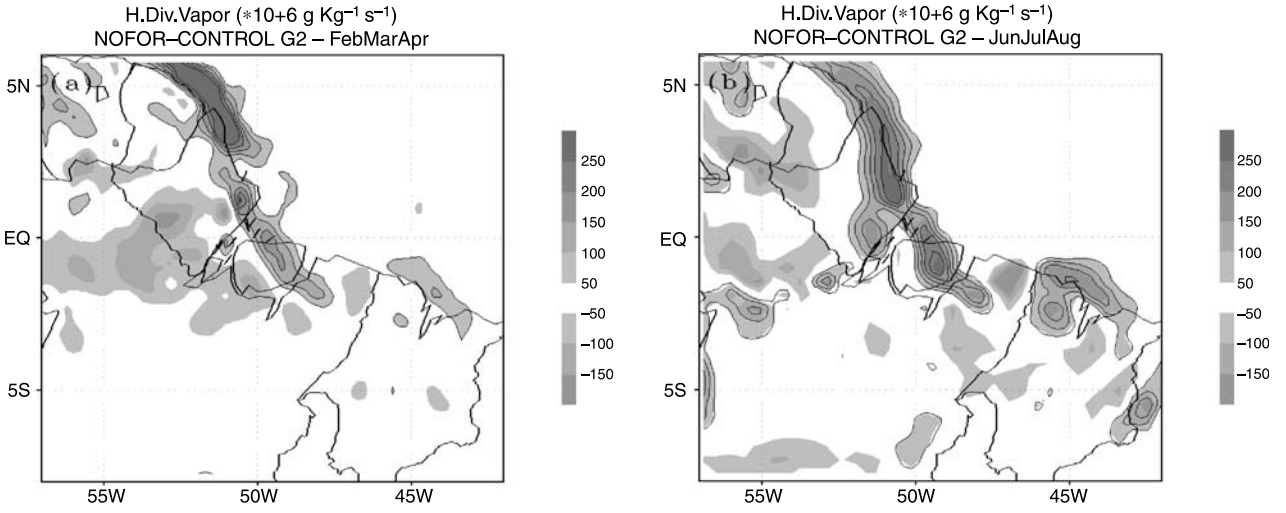

Fig. 11. The average humidity-divergence anomaly ($\times 10^6\,g\,kg^{-1}\,s^{-1}$) for: **a**) rainy months (February to April 2001) and; **b**) dry months (June to August 2001). Shading intervals are $50 \times 10^6\,g\,kg^{-1}\,s^{-1}$. Solid contours for positive values

(Fig. 10b). Because of the increased windspeeds near the surface, there was an anomalous humidity divergence along the coastline and increasing humidity convergence towards the interior of the continent (Fig. 11).

4. Summary and conclusions

Multiple effects of the eventual substitution of the forest by pasture over the eastern sub-region of Amazonia were predicted through the RAMS-model simulations. This mesoscale regional model incorporates a comprehensive physical representation of the radiative, convective, cloud microphysics, and surface-atmosphere interaction processes. Therefore, it is appropriate for studying the atmospheric responses to local variations in surface vegetation combined with the influence of the existing topography, land-ocean interfaces and large rivers of the region.

The results of this study, as with all other numerical modelling simulations, are highly dependent on the performance and limitations of the chosen model. These particular deforestation simulations revealed important effects that have not been previously investigated. For this

area, GCM studies have not simulated effects such as the influence of the large rivers in the region. Contrary to most large-scale model studies, the RAMS-model simulation predicted that the deforestation of eastern Amazonia would not produce a generalised reduction of precipitation over the region.

The present simulations indicated that deforestation would result in reduced cloud cover and precipitation over certain areas, such as the Amapá coast, the eastern part of Marajo Island and along the large rivers of this region. This would be particularly pronounced along the Amazon, near the city of Santarém. However, over the mountain slopes in central-southern Pará, as well as those north of the Amazon, increased cloud cover and precipitation were predicted. It should be mentioned that GCM simulations of South American upland regions produced a similar result (Manzi and Planton, 1996). In contrast, Hahmann and Dickinson (1997) showed that variations in humidity convergence and precipitation during the rainy season in Amazonia presented a shift in the area of maximum precipitation, rather than a generalised decrease over the deforested area.

The main contribution to the simulated precipitation values came from the RAMS explicit microphysics precipitation sub-module. This type of modelled precipitation dominates the anomaly field computed between the deforested run and the control run. Considering only the Kuo-type convective parameterisation of the model, comparison of the deforested and control runs revealed that there was a generalised increase in precipitation. The only exception was over a narrow coastal strip, where the biophysical parameters for vegetation were identical in the two simulations. Since Kuo-type convective parameterisation is dependent on the degree of thermodynamic instability of the atmosphere, this finding indicates that deforestation of Amazonia would result in an increase in the number of deep convective events, primarily over upland areas.

The sensible and latent heat fluxes also presented negative and positive anomaly regions resulting from deforestation. The magnitudes of these anomalies would be greater during the dry season. Qualitatively similar results have previously been simulated using GCMs (Nobre et al., 1991; Manzi and Planton, 1996). Over the deforested area south of the equator, a decrease in surface latent heat fluxes was predicted. However, over the upland areas of western Amapá and north-eastern Pará (corresponding to the regions of increased precipitation anomalies), deforestation would produce an increase in latent heat fluxes.

The results indicate that deforestation should produce a generalised increase in temperatures and a generalised decrease in the water vapour mixing ratio. The exception in both cases was the area along the Amazon, over the flood plains near Santarém. With the exception of the mesoscale spatial details, the amplitude variations in RAMS-simulated temperature increases and water vapour mixing ratio decreases are comparable to those obtained through GCM simulations (Nobre et al., 1991; Manzi and Planton, 1996).

Windspeed near the surface is the meteorological variable that undergoes the greatest positive variation attributable to deforestation. These variations are even more significant over the upwind side of the hills near the Atlantic coastline. The shift from forest to pasture reduces the surface roughness coefficient, which in turn allows windspeeds to increase and lessens humidity convergence over the ocean-land interface. Consequently, rainfall decreases in the area. It should be pointed out that the deforested simulation did not predict a significant increase in windspeeds over the Amazon flood plains surrounding Santarém.

In general, the high-resolution simulations of deforestation employed in this study reveal that topography, coastline profile and large rivers all play important roles in the anomalous patterns of precipitation, wind, and energy exchange in the eastern region of Amazonia.

Acknowledgements

This work was supported by the Brazilian Tropical Forests Protection Program (PPG7/FINEP/MCT – Grant No. 64.99.0425.00), by the Ministry of Science and Technology (MCT) and by the CNPq/PADCT Millennium Institutes Initiative (Project number 62.0056/01-0, and Project number 62.0065/01-0). The authors would like to thank Tiago Correa and Zilurdes Lopes for their help with, respectively, computation and text processing. We also thank the Centro de Previsão do Tempo e Estudos Climáticos (CPTEC) of the Instituto Nacional de Pesquisas Espaciais (INPE) for furnishing the

data from the automatic stations at Altamira and Marabá. Special thanks to the staff of the MASTER Laboratory of the Institute for Astronomy, Geophysics and Atmospheric Sciences of the University of São Paulo for their computational support for the RAMS model and for the meteorological data provided. The authors also wish to extend thanks to Dr. Regina Celia S. Alvalá who allowed access to the CPTEC/INPE data file on soil moisture content and vegetation used in this study. Finally, we express our gratitude for the constant encouragement provided by Dr. Carlos A. Nobre.

References

Cohen JCP, Silva Dias MAF, Nobre CA (1995) Environmental conditions associated with Amazonian squall lines: A case study. Mon Wea Rev 123: 3163–3174

Costa MR, Foley JA (2000) Combined effects of deforestation and doubled atmospheric CO_2 concentrations on the climate of Amazonia. J Climate 13: 18–34

Cotton WR, Pielke RA Sr, Walko RL, Liston GE, Tremback CJ, Jiang H, McAnelly RL, Harrington JY, Nicholls ME, Carrio GG, McFadden LP (2003) RAMS 2001: Current Status and future directions. Meteorol Atmos Phys 82: 5–29

Eltahir EAB (1996) Role of vegetation in sustaining large-scale atmospheric circulations in the tropics. J Geophys Res 101(D2): 4255–4268

Figueroa SN, Nobre CA (1990) Precipitation distribution over central and western tropical South America. Climanalise 5: 36–44

Freitas SR (1999) Numerical Modeling of the transport and emissions from biomass burning on South America tropical forest and savanna. Ph.D. Thesis – Institute of Physics, University of Sao Paulo, 204 pp (In Portuguese)

Garstang M, Massier HL Jr, Halverson J, Greco S, Scala J (1994) Amazon coastal squall lines, part I: Structure and kinematics. Mon Wea Rev 122: 608–622

Hahmann NA, Dickinson RE (1997) RCCM2-BATS Model over tropical South America: Applications to tropical deforestation. J Climate 10: 1944–1964

Hastenrath S (1997) Annual cycle of upper air circulation and convective activity over the tropical Americas. J Geophys Res 102(D4): 4267–4274

Horel JD, Hahmann NA, Geisler JE (1989) An investigation of the annual cycles of convective activity over the tropical South America. J Climate 2: 1388–1403

Kousky VE (1980) Diurnal rainfall variation in Northeast Brazil. Mon Wea Rev 108: 488–498

Lean J, Bunton CB, Nobre CA, Rowntree RL (1996) The simulated impact of Amazonian deforestation on climate using measured ABRACOS vegetation characteristics. In: Gash JHC, Nobre CA, Roberts JM, Victoria RL (eds) Amazonian deforestation and climate. Chichester: Wiley, pp 549–576

Liston GE, Pielke RA Sr (2001) A climate version of the regional atmospheric modeling system. Theor Appl Climatol 68: 155–173

Lu LX, Pielke RA, Liston GE, Parton WJ, Ojima D, Hartman M (2001) Implementation of a two-way interactive atmospheric and ecological model and its application to the central United States. J Climate 14: 900–919

Manzi AO, Planton S (1996) A simulation of Amazonian deforestation using a GCM calibrated with ABRACOS and ARME data. In: Gash JHC, Nobre CA, Roberts JM, Victoria RL (eds) Amazonian deforestation and climate. Chichester: Wiley, pp 505–529

Marengo JA (1992) Interannual variability of surface climate in the Amazon basin. Int J Climatol 12: 853–863

Marengo JA, Liebmann B, Kousky VE, Filizola NP, Waier IC (2001) Onset and end of the rainy season in the Brazilian Amazon Basin. J Climate 14: 833–852

Miranda AC, Miranda HS, Lloyd J, Grace J, McIntyre JA, Meir P, Riggan P, Lockwood R, Brass J (1996) Carbon dioxide fluxes over a cerrado *sensu stricto* in central Brazil. In: Gash JHC, Nobre CA, Roberts JM, Victoria RL (eds) Amazonian deforestation and climate. Chichester: Wiley, pp 353–363

Negri AJ, Anagnostou EN, Adler RF (2000) A 10-yr climatology of Amazonian rainfall derived from passive microwave satellite observation. J Appl Meteor 39: 42–56

Nobre CA, Sellers PJ, Shukla J (1991) Amazonian deforestation and regional climate change. J Climate 4: 957–988

Pielke RA, Cotton WR, Walko RL, Tremback CJ, Lyons WA, Grasso LD, Nicholls ME, Moran MD, Wesley DA, Lee TJ, Copeland JH (1992) A comprehensive meteorological modeling system – RAMS. Meteorol Atmos Phys 49: 69–91

Polcher J (1995) Sensitivity of tropical convection to land surface processes. J Atmos Sci 52: 3143–3161

Polcher J, Laval K (1994) A statistical study of the regional impact of deforestation on climate in the LMD GCM. Climate Dynamics 10: 205–219

Rao VB, Hada K (1990) Characteristics of rainfall over Brazil: annual variations and connections with the Southern Oscillation. Theor Appl Climatol 42: 81–91

Rao VB, Cavalcanti IFA, Hada K (1996) Annual variations of rainfall over Brazil and water vapor characteristics of South America. J Geophys Res 101(D21): 26539–26551

Rossato L, Alvalá RCS, Tomasella J (2002) Climatology of soil humidity in Brazil. Pre-prints, 12th Brazilian Congress of Meteorology, Foz do Iguaçu, Paraná, SBMET, 4–9 August, 1910–1915. (In Portuguese)

Sestini MF, Alvalá RCS, Mello EMK, Valeriano DM, Chan CS, Nobre CA, Paiva JAC, Reimwe ES (2002) Vegetation maps development for use in meteorological and hydrological models. Instituto Nacional de Pesquisas Espaciais, Publicação INPE-8972-RPQ/730, São José dos Campos, 74 pp. (In Portuguese)

Silva Dias MAF, Silva Dias PL, Longo M, Fitzjarrald DR, Denning AS (2004) River breeze circulation in eastern Amazonia: observations and modelling results. Theor Appl Climatol (this issue)

Silva Dias MAF, Regnier P (1996) Simulation of mesoscale circulations in a deforested area of Rondônia in dry season. In: Gash JHC, Nobre CA, Roberts JM, Victoria RL (eds) Amazonian deforestation and climate. Chichester: Wiley, pp 531–547

Souza JRS, Lopes ZF, Cohen JCP, Costa ACL (2002) Variability of temperature and soil humidity in forests, pasture and mangroves in eastern Amazonia. Pre-prints, 12th Brazilian Congress of Meteorology, Foz do Iguaçu, Paraná, SBMET, 4–9 August, 2522–2528. (In Portuguese)

Tremback CJ (1990) Numerical simulation of a mesoscale convective complex: Model development and numerical results. *Ph.D. dissertation*, Atmosphere Science Paper No. 465, Department of Atmospheric Science, Colorado State University, 247 pp

Tripoli GJ, Cotton WR (1982) The Colorado State University three-dimensional cloud/mesoscale model – 1982, Part I: General theoretical framework and sensitivity experiments. J Rech Atmos 16: 185–220

Walko RL, Band LE, Baron J, Kittel TGE, Lammers R, Lee TJ, Ojima D, Pielke RA, Taylor C, Tague C, Tremback CJ, Vidale PL (2000) Coupled atmosphere-biophysics-hydrology models for environmental modeling. J Appl Meteor 39: 931–944

Walko RL, Cotton WR, Meyers MP, Harrington JH (1995) New RAMS cloud microphysics parameterization, Part I: the single-moment scheme. Atmos Res 38: 29–62

Wang H, Fu R (2002) Cross-equatorial flow and seasonal cycle of precipitation over South America. J Climate 15: 1591–1608

Werth D, Avissar R (2002) The local and global effects of Amazon deforestation. J Geophys Res 107(D20): art no. 8087

Wright IR, Nobre CA, Tomasella J, da Rocha HR, Roberts JM, Vertamatti E, Culf AD, Alvalá RCS, Hodnett MG, Ubarana VN (1996) Towards a GCM surface parameterization for Amazonia. In: Gash JHC, Nobre CA, Roberts JM, Victoria RL (eds) Amazonian deforestation and climate. Chichester: Wiley, pp 474–504

Authors' addresses: Dr. Adilson Wagner Gandu (e-mail: adwgandu@model.iag.usp.br), Institute of Astronomy, Geophysics and Atmospheric Sciences, University of São Paulo, Rua do Matão, 1226 – Cid. Universitária, 05508-090 São Paulo, SP, Brazil; Julia C. P. Cohen, José Ricardo S. de Souza, Department of Meteorology, Federal University of Pará, Belém, Brazil.